Journal of Hydrology 486 (2013) 211–223

Contents lists available at SciVerse ScienceDirect

Journal of Hydrology

journal homepage: www.elsevier.com/locate/jhydrol

3D analysis of geometry and flow changes in a limestone fracture during dissolution

Catherine Noiriel [a,*], Philippe Gouze [b], Benoît Madé [c]

[a] Géosciences Environnement Toulouse (GET), Observatoire Midi-Pyrénées, Université Paul Sabatier, CNRS, IRD, 31400 Toulouse, France
[b] Géosciences Montpellier, UMR 5243, CNRS, Université de Montpellier II, 34095 Montpellier, France
[c] Agence Nationale pour la gestion des Déchets Radioactifs, 92298 Châtenay Malabry, France

ARTICLE INFO

Article history:
Received 20 July 2012
Received in revised form 5 December 2012
Accepted 26 January 2013
Available online 14 February 2013
This manuscript was handled by Laurent Charlet, Editor-in-Chief, with the assistance of Tamotsu Kozaki, Associate Editor

Keywords:
Fracture
X-ray micro-tomography
Dissolution
CO_2
Limestone
Flow modelling

SUMMARY

The effects of reactive transport on fracture geometry and fluid flow were investigated through an integrated experimental and modelling approach. A fractured limestone sample (90% calcite) was injected with an acidic CO_2-rich solution over a period of 55 h to induce carbonate dissolution. The changes in fracture geometry and related parameters are reported for six data sets obtained from synchrotron X-ray micro-tomography experiments. A series of algorithms was used to extract the aperture and fracture walls from 3D images and allowed quantification of the geometry changes with an optical resolution of 4.91 μm. In addition, measurement of fluid chemistry, hydraulic tests and computation of Navier–Stokes flow constrained the characterisation of the dissolution process. The effects of reactive transport on fracture geometry and fluid flow were then discussed. The presence of silicates in the rocks led to heterogeneous dissolution at the micro-scale, despite dissolution appearing to be quite homogeneous at sample-scale. No formation of preferential flow pathways was noticed, although heterogeneous dissolution at the micro-scale led to fracture walls and aperture decorrelation, and to modification of the flow velocity profiles in the fracture.

1. Introduction

Fractures control the flow and transport of fluids and pollutants in low-permeability rocks. Assessing long-term transport of contaminants in fractured rocks is essential, especially regarding nuclear waste storage, geothermal energy or CO_2 sequestration in reservoirs. For these situations, long-lasting flow of fluids in disequilibrium with the rock is expected and dissolution (or precipitation) processes can quickly and deeply alter the geometry of fractures, and, as a consequence, their hydraulic and transport properties, such as permeability and dispersivity. For instance, karst formation in limestone is certainly the most remarkable example of alteration of flow and transport properties over a relatively short period of time. It is probable that in many geological and environmental applications, fracture parameters must be considered as variables. Yet, the prediction of flow and transport changes in fractures undergoing chemical reactions is challenging due to the complexity of fluid–rock interactions and the possible triggering of positive (or negative) feedbacks.

Fractures are heterogeneous structures, the macroscopic physical properties of which depend on local characteristics. For instance, fracture permeability and transport properties are closely related to the microstructure, such as physico-chemical properties and spatial distribution of the rock-forming minerals, fracture wall roughness, tortuosity, and contacting asperities. Aperture distribution and anisotropy are also main parameters in determining the flow and transport properties. Therefore, fracture geometry determination is important to model flow and transport accordingly.

The control of various fracture parameters on fluid flow (Appendix A) and of transport of solutes (Appendix B) into fractures has been discussed extensively. However, discrepancies between numerical models and natural configurations are still expected because numerical models often idealise the fracture geometry or take into account the presence of only one reactive mineral, despite rocks are rarely being mono-mineral. The advent of non-invasive and non-destructive techniques has improved in situ characterisation of fracture geometry (Bertels and DiCarlo, 2001; Keller, 1998; Vandersteen et al., 2003) and flow (Dijk et al., 1999; Karpyn et al., 2007; Kumar et al., 1997), which now appear to be very pertinent for observing changes during dynamic experiments (Detwiler, 2008; Detwiler et al., 2003; Dijk et al., 2002; Ellis et al., 2011; Enzmann et al., 2004; Gouze et al., 2003; Landis et al., 2003; Noiriel et al., 2007a, 2007b). Experimental effort, including direct permeability and geometry measurements, is still required to predict the long-term evolution of such heterogeneous systems.

The present study aims to characterise fracture geometry and flow changes during a flow-through dissolution experiment in a

* Corresponding author. Address: Géosciences Environnement Toulouse (GET), UMR 5533, Université Paul Sabatier, CNRS, IRD, CNES, 14, avenue Edouard Belin, 31400 Toulouse, France. Tel.: +33 561 332 589; fax: +33 561 332 560.
E-mail address: catherine.noiriel@get.obs-mip.fr (C. Noiriel).

0022-1694/$ - see front matter © 2013 Elsevier B.V. All rights reserved.
http://dx.doi.org/10.1016/j.jhydrol.2013.01.035

slightly argillaceous limestone sample. By developing a technique to measure repetitively the fracture void geometry, a direct comparison can be made between geometrical and hydraulic property changes and the dissolution process. X-ray micro-tomography allowed the collection of the different parameters describing the changes in fracture geometry both before the experiment and after different stages of dissolution. The effects of dissolution on the fracture geometry were characterised after extraction of the two fracture walls and the aperture from 3D image volumes. Measurement of fluid chemistry and permeability complementary constrained the characterisation of the dissolution process. In addition, fluid flow was computed in the fracture and the resulting hydraulic aperture ($a_{h\text{-}NS}$) was compared with three others independent experimental measurements of the fracture aperture, i.e. hydraulic aperture (a_h) determined from hydraulic tests, mechanical aperture (a_m) determined from XMT, and chemical aperture (a_c) determined from mass balance calculation. Finally, the implication of aperture increase and rock mineralogy, flow, transport and geometry changes will be discussed.

2. Experimental procedure

2.1. Sample characteristics

The flow-through experiment was carried out using a slightly argillaceous limestone that contains about 10% of silicate minerals (principally clays, with a minor amount of quartz) and less than 1% of iron oxides. The carbonate matrix is essentially composed of partially recrystallized micro-crystalline calcite and to a minor extent by biogenic fragments crystallised in sparite.

A cylindrical sample of 15 mm in length and 9 mm in diameter was artificially fractured using a Brazilian-like test to produce a longitudinal fracture parallel to the cylinder axis. The two fracture walls were put together and sealed with epoxy resin on their edges to prevent any mechanical displacements of the fracture walls during experiment. The external surface of the fractured sample apart from the fracture inlet and outlet was also covered with epoxy resin to avoid dissolution.

2.2. Flow-through experiment

The inlet fluid used in the experiment was a 0.010 ± 0.001 M NaCl solution prepared from reagent-grade salt diluted in deionised water. The fluid, initially degassed, was maintained at equilibrium with CO_2 at a partial pressure of 0.10 ± 0.01 MPa during the experiment.

After vacuum saturation with deionised water, the sample was injected with the inlet fluid using a dual piston pump at a controlled flow rate of 100 $cm^3\ h^{-1}$ ($2.78 \times 10^{-8}\ m^3\ s^{-1}$). The confining pressure was equal to the pressure at the sample inlet. The pressure at the outlet was maintained at 0.13 MPa using a calibrated back-pressure controller to avoid CO_2 degassing during the experiment.

Permeability was calculated from the differential pressure record between the sample inlet and outlet (ΔP) using the steady-state flow method (Eq. (A.2)), initially ($t = t_0$) and at the end of each stage of dissolution, i.e. after 8 h (t_1), 16 h (t_2), 28 h (t_3), 37 h (t_4) and 55 h (t_5) from the start of the experiment.

Both the inlet and outlet *pH* were recorded continuously to detect either potential CO_2 saturation changes of the inlet fluid or variation of the alkalinity of the outlet solution. The outlet solution was also sampled repeatedly for major and minor ions analysis by ICP-AES (inductive coupled plasma-atomic emission spectroscopy). A schematic representation of the flow-through experiment is presented in Fig. 1a.

2.3. Geometry characterisation using synchrotron X-ray micro-tomography

2.3.1. X-ray tomography imaging of the fracture

The geometry of the fracture was obtained after processing of the XMT data sets acquired at the European Synchrotron Radiation Facility ID19 beam-line (Grenoble, France). A total of six data sets were collected at times t_0 to t_5. The XMT method provides non-invasive and non-destructive visualisation and characterisation of the 3D sample from around a thousand 2D radiographs of the X-ray attenuation properties of the various materials forming the sample. As air in the fracture void and minerals in the rock matrix have different X-ray attenuation properties, they can be differentiated on the 3D images.

The X-ray source was diffracted through a double Si(1 1 1) crystal yielding a focused monochromatic and parallel beam with energy of 40 keV. The combination of an adapted optics with the CCD camera provides a spatial resolution of 6 μm for an optical resolution (pixel size) of 4.91 μm. As the camera field is shorter than the height of the sample, only the upper part of the sample close to the inlet was scanned (Fig. 1b). Volume reconstruction was carried out from nine hundred 2048 × 2048 radiographs using direct Fourier inversion, through the use of a filtered back-projection algorithm (Herman, 1980). Radiographs were filtered prior to the reconstruction in order to eliminate the random noise due to high-energy diffracted photons, by substituting these noisy pixels with the median of their neighbours. The reconstruction provided six 3D image volumes of the X-ray absorption by the different materials in the sample, named V_0 to V_5. Each volume is about 400 × 2000 × 1600 voxels of volume 4.91 × 4.91 × 4.91 μm^3 each.

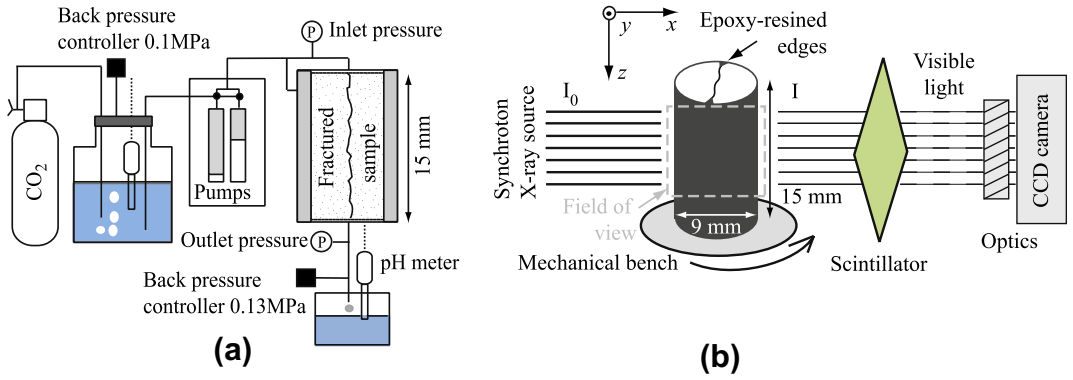

Fig. 1. (a) Schematic representation of the plug-flow apparatus and (b) field of view (10 × 10 mm) covered during X-ray micro-tomography imaging.